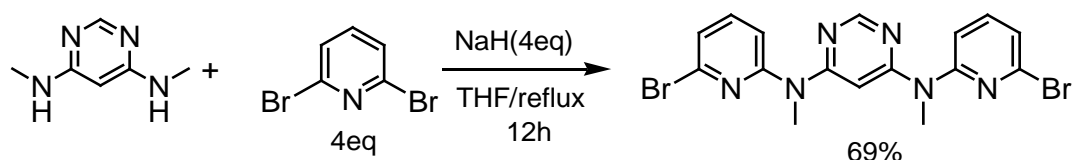


Electronic Supplementary Information

Synthesis of 1,3,5-alternate azacalix[3]pyridine[3]pyrimidine and its complexation with fullerenes via multiple π/π and CH/ π interactions

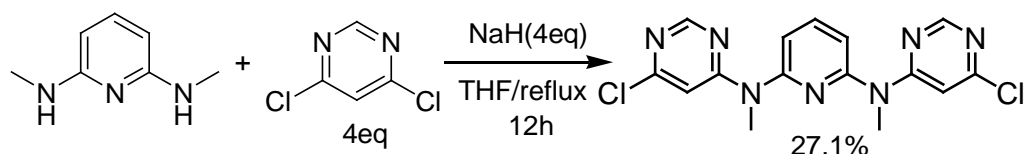
1. Synthesis of azacalix[3]pyridine[3]pyrimidine 3

1.1. Synthesis of fragment 1



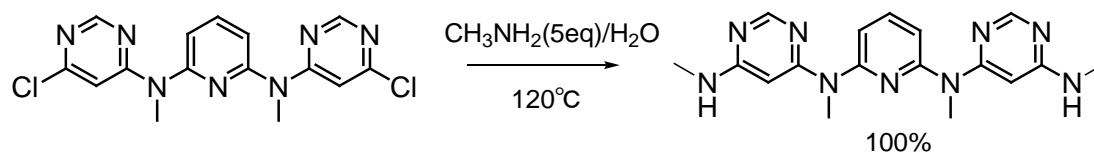
To a solution of 4,6-bis(methylamino)pyrimidine (1.38 g, 10 mmol) in dry THF (60 mL) at room temperature was added NaH (0.96 g, 40 mmol) slowly and the mixture was heated to reflux. After 10 h, 2,6-dibromopyridine (9.48 g, 40 mmol) was added to the mixture slowly and the reaction mixture was refluxed for another 12 h. The reaction mixture was then cooled down to room temperature and water (1 mL) was added slowly. The solvent was removed under reduced pressure, and the residue was dissolved in CH_2Cl_2 (200 mL). The organic solution was washed with brine (3×50 mL) and dried over with anhydrous MgSO_4 . After removal of solvent, the residue was chromatographed on a silica gel column (100-200) with a mixture of petroleum ether and ethyl acetate as the mobile phase to give pure **1** (3.09 g, 69%): mp 203-204 °C, IR (KBr) ν 1608, 1580, 1552, 1438, 1167 cm^{-1} ; ^1H NMR (300 MHz, CDCl_3) δ 8.56 (s, 1H), 7.56 (t, $J = 7.8$ Hz, 2H), 7.32 (d, $J = 8.1$ Hz, 2H), 7.19 (d, $J = 7.5$ Hz, 2H), 6.84 (s, 1H), 3.61 (s, 6H); ^{13}C NMR (75 MHz, CDCl_3) δ 161.7, 157.3, 156.3, 139.71, 139.68, 122.6, 115.4, 93.5, 35.8; MS (CI) m/z (%) 452 $[\text{M}+4]^+$ (69), 450 $[\text{M}+2]^+$ (85), 449 $[\text{M}+1]^+$ (100), 371 $[\text{M}-\text{Br}]^+$ (51); Anal. Calcd for $\text{C}_{16}\text{H}_{14}\text{Br}_2\text{N}_6$: C, 42.69; H, 3.13; N, 18.67. Found: C, 42.22; H, 3.17; N, 18.31.

1.2. Synthesis of fragment 2



Synthesis of N_2,N_6 -bis(6-chloropyrimidin-4-yl)- N_2,N_6 -dimethylpyridine-2,6-diamine. N_2,N_6 -bis(6-chloropyrimidin-4-yl)- N_2,N_6 -dimethylpyridine-2,6-diamine was prepared from 2,6-bis(methylamino)pyridine by a similar procedure as that for the synthesis of **1**. The reaction of 2,6-bis(methylamino)pyridine (1.37 g, 10 mmol) with 4,6-dichloropyrimidine (5.96 g, 40 mmol) with

the aid of NaH (0.96 g, 40 mmol) gave product as a white solid (977 mg, 27%): mp 150-151 °C, IR (KBr) ν 1603, 1564, 1524, 1442, 1353 cm^{-1} ; ^1H NMR (300 MHz, CDCl_3) δ 8.58 (s, 2H), 7.83 (t, $J = 7.8$ Hz, 1H), 7.21 (d, $J = 8.1$ Hz, 2H), 7.02 (d, $J = 0.6$ Hz, 2H), 3.61 (s, 6H); ^{13}C NMR (75 MHz, CDCl_3) δ 162.3, 160.1, 158.1, 154.6, 140.1, 114.9, 105.8, 36.0; MS (CI) m/z (%) 364 $[\text{M}+2]^+$ (100), 362 $[\text{M}]^+$ (53); Anal. Calcd for $\text{C}_{15}\text{H}_{13}\text{Cl}_2\text{N}_7$: C, 49.74; H, 3.62; N, 27.07. Found: C, 49.52; H, 3.68; N, 26.96.



Synthesis of 2

An autoclave equipped with a magnetic stir bar was charged with N_2,N_6 -bis(6-chloropyrimidin-4-yl)- N_2,N_6 -dimethylpyridine-2,6-diamine (2.25 g, 5 mmol) and 10 mL methylamine aqueous solution (25-30%). Then it was heated to 120 °C for 10 h. After the mixture was cooled to room temperature, dichloromethane (100 mL) was added, and the organic phase was washed with brine (3 \times 50 mL). The aqueous phase was re-extracted with dichloromethane (3 \times 20 mL), and the combined organic phase was dried over anhydrous MgSO_4 . After removal of solvent, the residue was chromatographed on a silica gel column with a mixture of petroleum ether and ethyl acetate as the mobile phase to give pure **2** (1.76 g, 100%) as a white solid: mp 203-204 °C, IR (KBr) ν 3244, 1601, 1568, 1433, 1150 cm^{-1} ; ^1H NMR (300 MHz, CDCl_3) δ 8.30 (s, 2H), 7.61 (t, $J = 8.1$ Hz, 1H), 7.09 (d, $J = 8.1$ Hz, 2H), 6.02 (s, 2H), 4.74 (s, br, 2H), 3.57 (s, 6H), 2.85 (d, $J = 5.1$ Hz, 6H); ^{13}C NMR (75 MHz, CDCl_3) δ 163.7, 162.2, 157.5, 155.4, 138.5, 112.3, 85.7, 35.6, 28.4; MS (CI) m/z 352 $[\text{M}]^+$; Anal. Calcd for $\text{C}_{17}\text{H}_{21}\text{N}_9$: C, 58.10; H, 6.02; N, 35.87. Found: C, 57.61; H, 5.98; N, 35.70.

1.3. Synthesis of methylazacalix[3]pyridine[3]pyrimidine 3. Under argon protection, a mixture of **1** (1 mmol) and **2** (1 mmol), $\text{Pd}_2(\text{dba})_3$ (138 mg, 0.15 mmol), dppp (123 mg, 0.3 mmol), and sodium *tert*-butoxide (288 mg, 3 mmol) in anhydrous 1,4-dioxane (200 mL) was refluxed for 2 h. The reaction mixture was cooled down to room temperature and filtered through a Celite pad. The filtrate was concentrated under vacuum and the residue was dissolved in dichloromethane (100 mL) and washed with brine (3 \times 25 mL). The aqueous phase was re-extracted with dichloromethane

(3×20 mL), and the combined organic phase was dried over anhydrous MgSO₄. After removal of solvent, the residue was chromatographed on a silica gel column with a mixture of petroleum ether and ethyl acetate (1:10) as the mobile phase to give product **3** (466 mg, 73%) as colourless needles: mp >300 °C; IR (KBr) ν 1601, 1565, 1525, 1429 cm⁻¹; ¹H NMR (300 MHz, CDCl₃) δ 8.61 (d, *J* = 0.6 Hz, 3H), 7.38 (t, *J* = 8.1 Hz, 3H), 6.77 (d, *J* = 8.1 Hz, 6H), 6.47 (s, 3H), 3.57 (s, 18H); ¹³C NMR (75 MHz, CDCl₃) δ 162.1, 158.8, 156.2, 137.8, 111.6, 92.3, 34.9; MS (MALDI-TOF) *m/z* 662 [M+Na]⁺, 640 [M+H]⁺. Anal. Calcd. for C₃₃H₃₃N₁₅: C, 61.96; H, 5.20; N, 32.84. Found: C, 61.99; H, 5.20; N, 32.80. Slow evaporation (2 to 3 days) of the solvent from the solution of **3** in CH₂Cl₂ and MeOH at room temperature gave single crystals of **3**. The single crystals of complex [**3**₂·C₆₀] were obtained through a diffusion method by layering a C₆₀ solution in toluene (2 ml) over a solution of **3** in CHCl₃ (2 ml).

2. Fluorescence titration of **3** with C₆₀ and C₇₀

The fluorescence titrations were performed on a Hitachi F-4500 spectrometer. The excitation wavelength was 333 nm, excitation and emission slits were set at 10 nm and 5 nm, respectively. The scan speed was 240 nm/min. To a graduated cuvette containing **3** in toluene (1.6×10⁻⁶ mol.dm⁻³), quantitative solutions of C₆₀ or C₇₀ in toluene were added. Fluorescence intensity was recorded after the mixed solution was stayed for 12 hours. The titrations were repeated for three times.

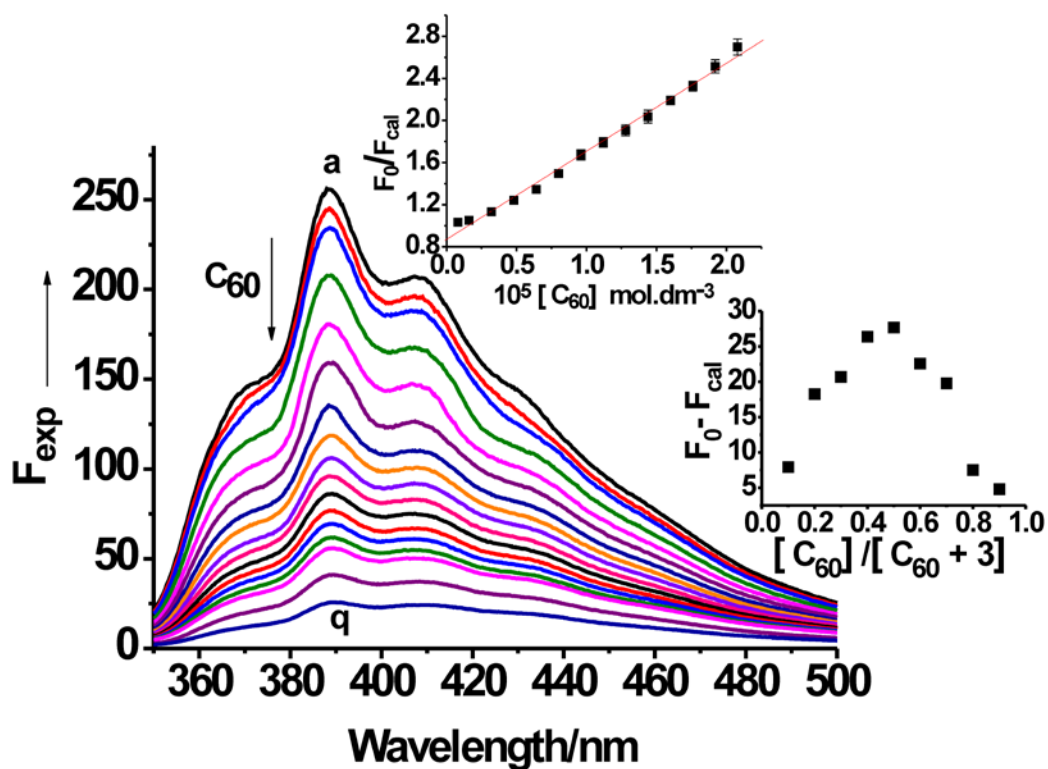


Figure S1. Fluorescence titration of **3** with C_{60} . Upper insertion is variations of fluorescence intensity F_o/F_{cal} of **3** with increasing C_{60} concentration and lower insertion is the Job's plot. Emission spectra ($\lambda_{ex} = 333$ nm) of **3** (1.6×10^{-6} mol.dm $^{-3}$) in the presence of C_{60} in toluene at 25 °C. The concentrations of C_{60} for curves a-q (from top to bottom) are 0, 0.80, 1.60, 3.20, 4.80, 6.40, 8.00, 9.60, 11.2, 12.8, 14.4, 16.0, 17.6, 19.2, 20.8, 25.6, 32.0 ($\times 10^{-6}$ mol.dm $^{-3}$). The Job plot was measured for **3**- C_{60} complex in toluene solution ($[3] + [C_{60}] = 6.4 \times 10^{-6}$ mol.dm $^{-3}$). Association constant ($K_{a(1:1)}$) of $(8.28 \pm 0.11) \times 10^4$ M $^{-1}$ was calculated using the Hyperquad 2000 program.

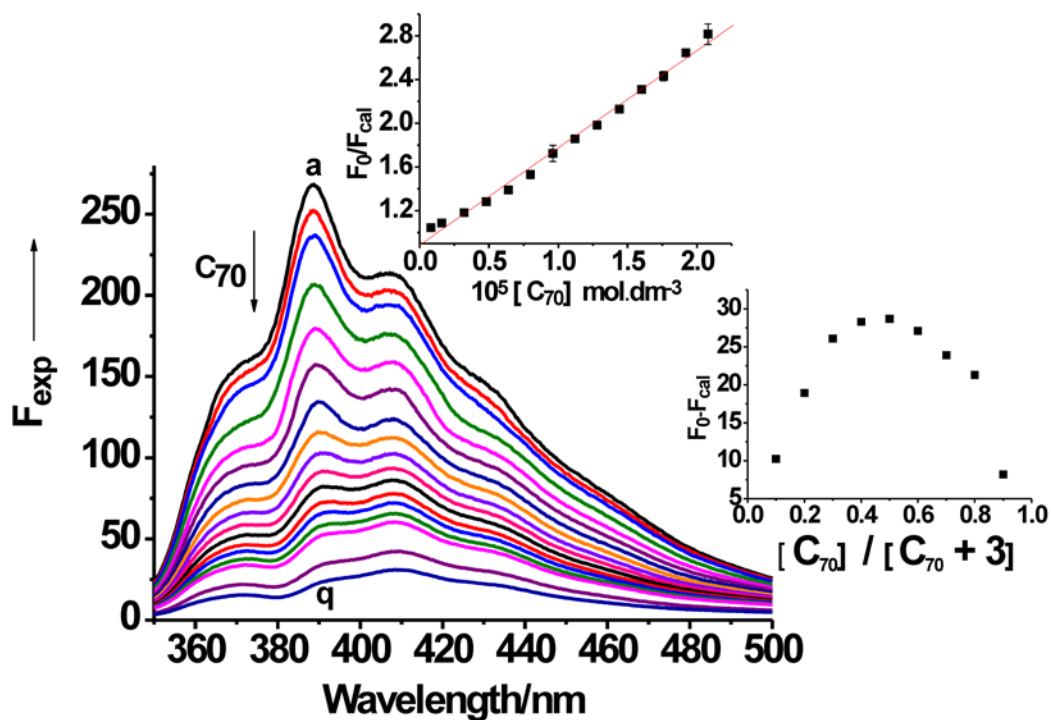


Figure S2. Fluorescence titration of **3** with C_{70} . Upper insertion is variations of fluorescence intensity F_0/F_{cal} of **3** with increasing C_{70} concentration and lower insertion is the Job's plot. Emission spectra ($\lambda_{ex} = 333 \text{ nm}$) of **3** ($1.6 \times 10^{-6} \text{ mol.dm}^{-3}$) in the presence of C_{70} in toluene at 25°C . The concentrations of C_{70} for curves a-q (from top to bottom) are 0, 0.80, 1.60, 3.20, 4.80, 6.40, 8.00, 9.60, 11.2, 12.8, 14.4, 16.0, 17.6, 19.2, 20.8, 25.6, 32.0 ($\times 10^{-6} \text{ mol.dm}^{-3}$). The Job plot was measured for **3**- C_{70} complex in toluene solution ($[3] + [C_{70}] = 6.4 \times 10^{-6} \text{ mol.dm}^{-3}$). Association constant ($K_{a(1:1)}$) of $(8.83 \pm 0.07) \times 10^4 \text{ M}^{-1}$ was calculated using the Hyperquad 2000 program.

3. X-ray crystal structure of $[3_2.C_{60}]$

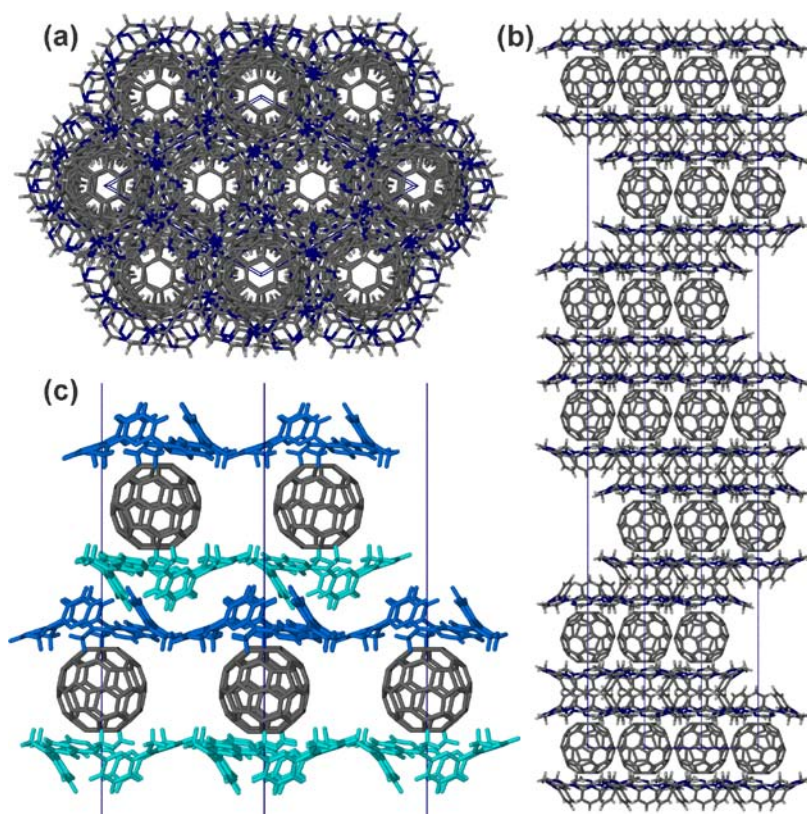


Figure S3. Packing view of the $[3_2 \cdot C_{60}]$ adduct along (a) the c axis and (b) the $[2\ 1\ 0]$ direction and (c) the $[1\ 1\ 0]$ direction .

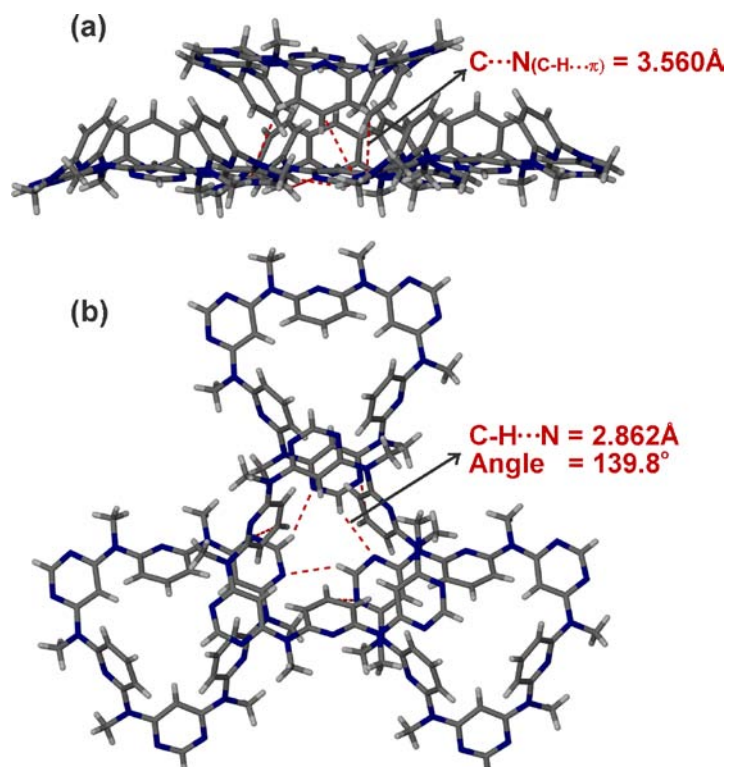


Figure S4. The weak interaction bonded aggregate in the crystal of **3** and $[3_2 \cdot C_{60}]$ adduct.

4. DFT calculation

The X-ray molecular structure of macrocyclic host of the complex $[3_2.C_{60}]$ was used to calculate the electrostatic potential distribution of azacalix[3]pyridine[3]pyrimidine. As shown in Figure S4, the pyrimidine rings and the pyridine nitrogen atoms, which are most electron negative (in red), form a concave complimentary to the convex of C_{60} , enabling multiple and strong intramolecular π/π interactions with C_{60} . The six methyl groups on the bridging positions, which are electron positive in nature (in blue), are in the positions able to form weak CH/π interactions with C_{60} .

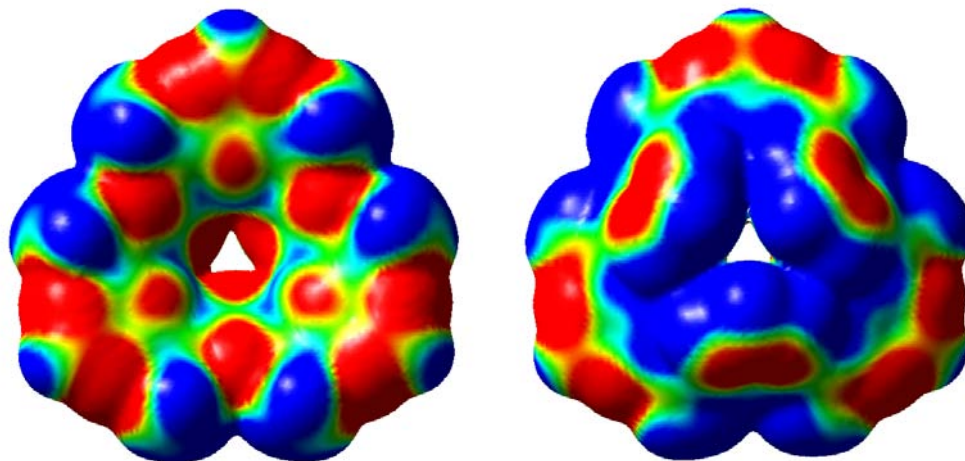
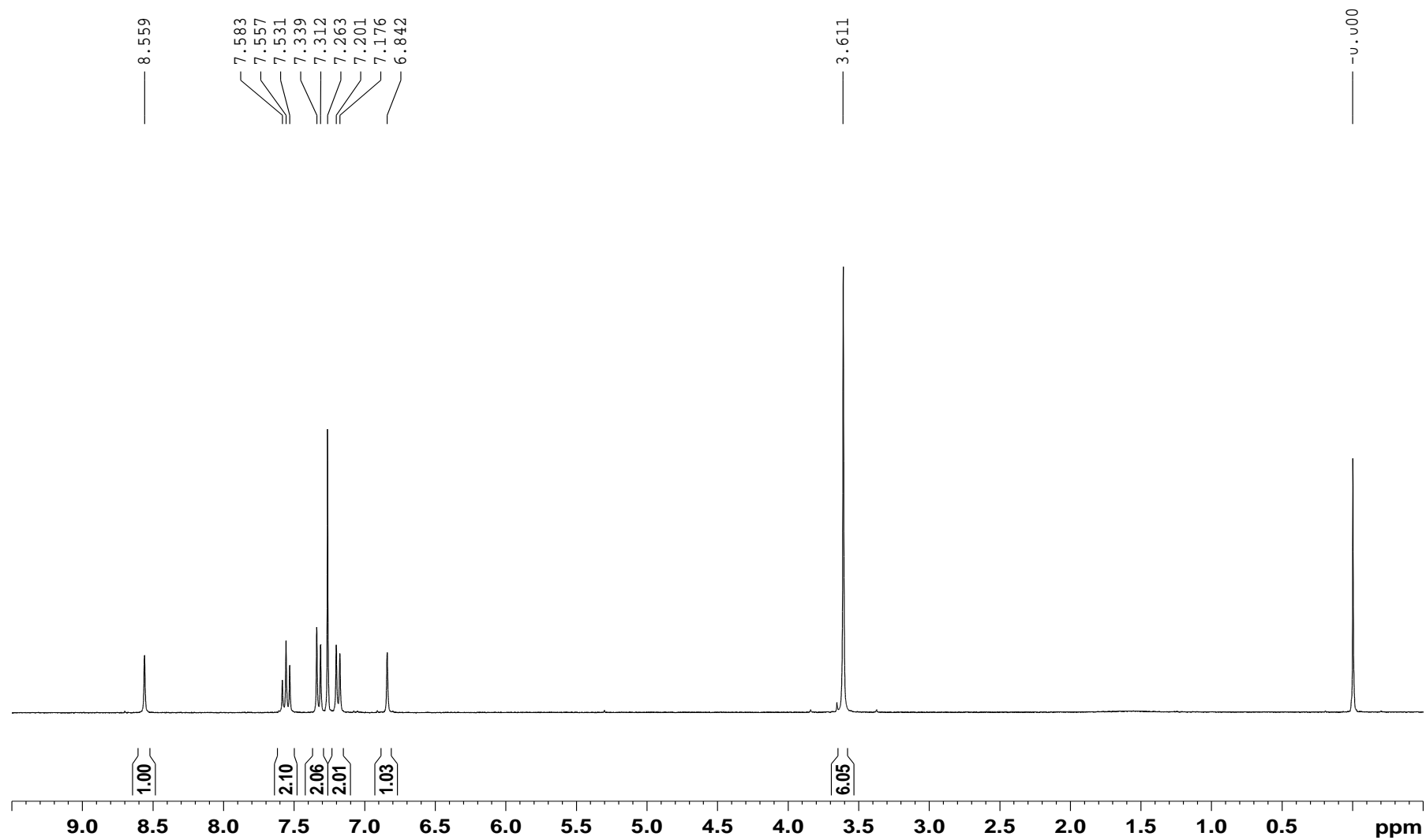
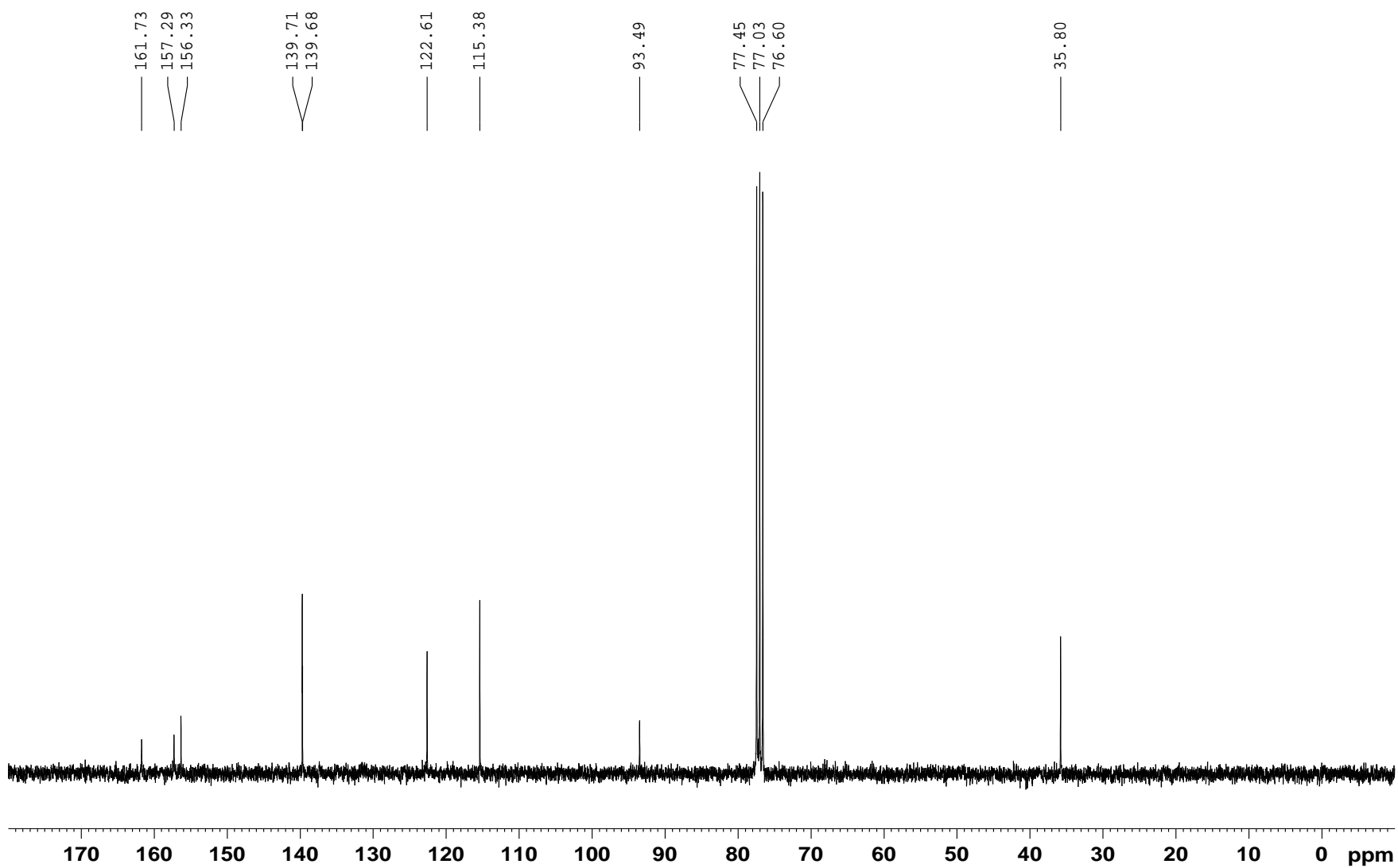
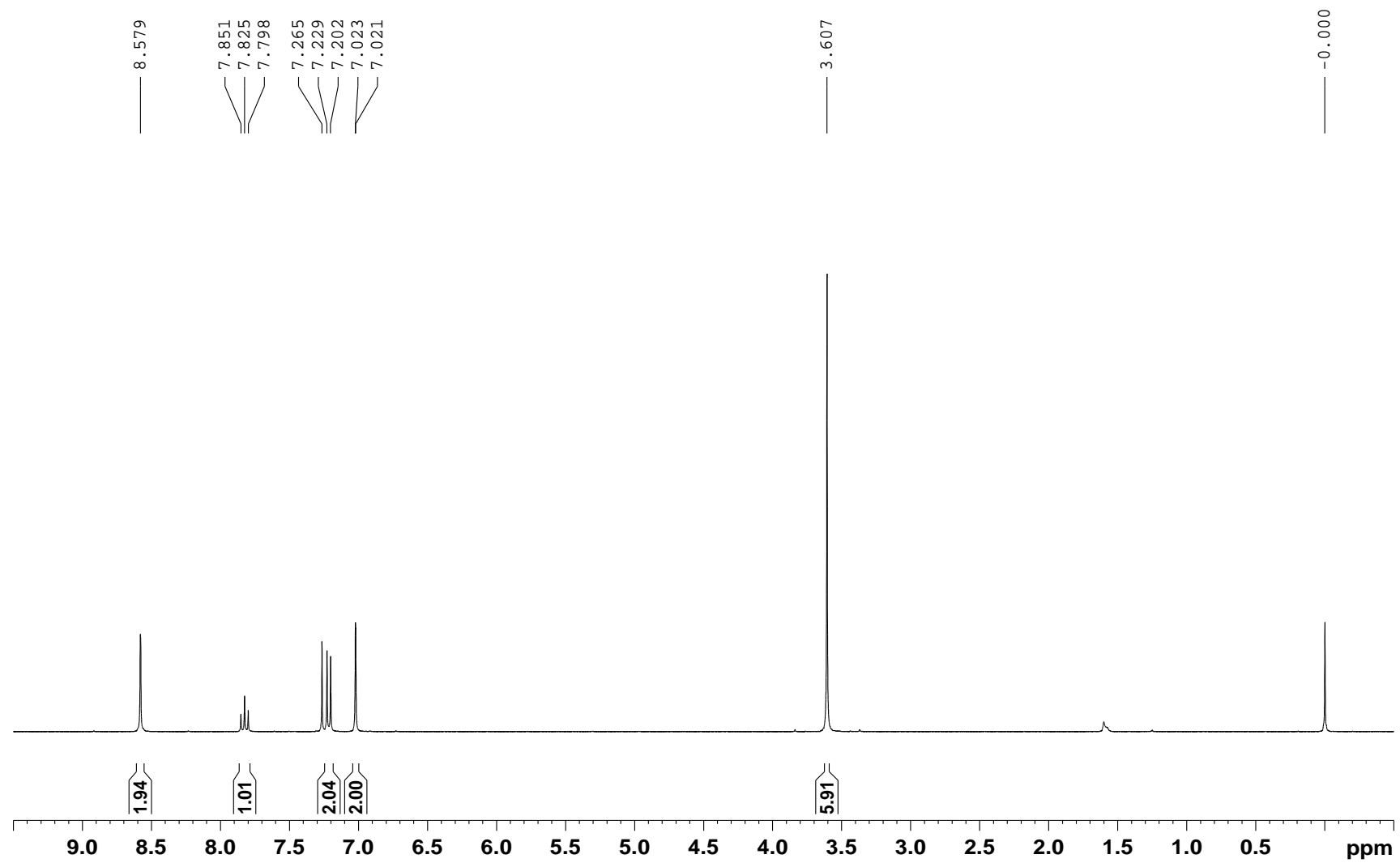


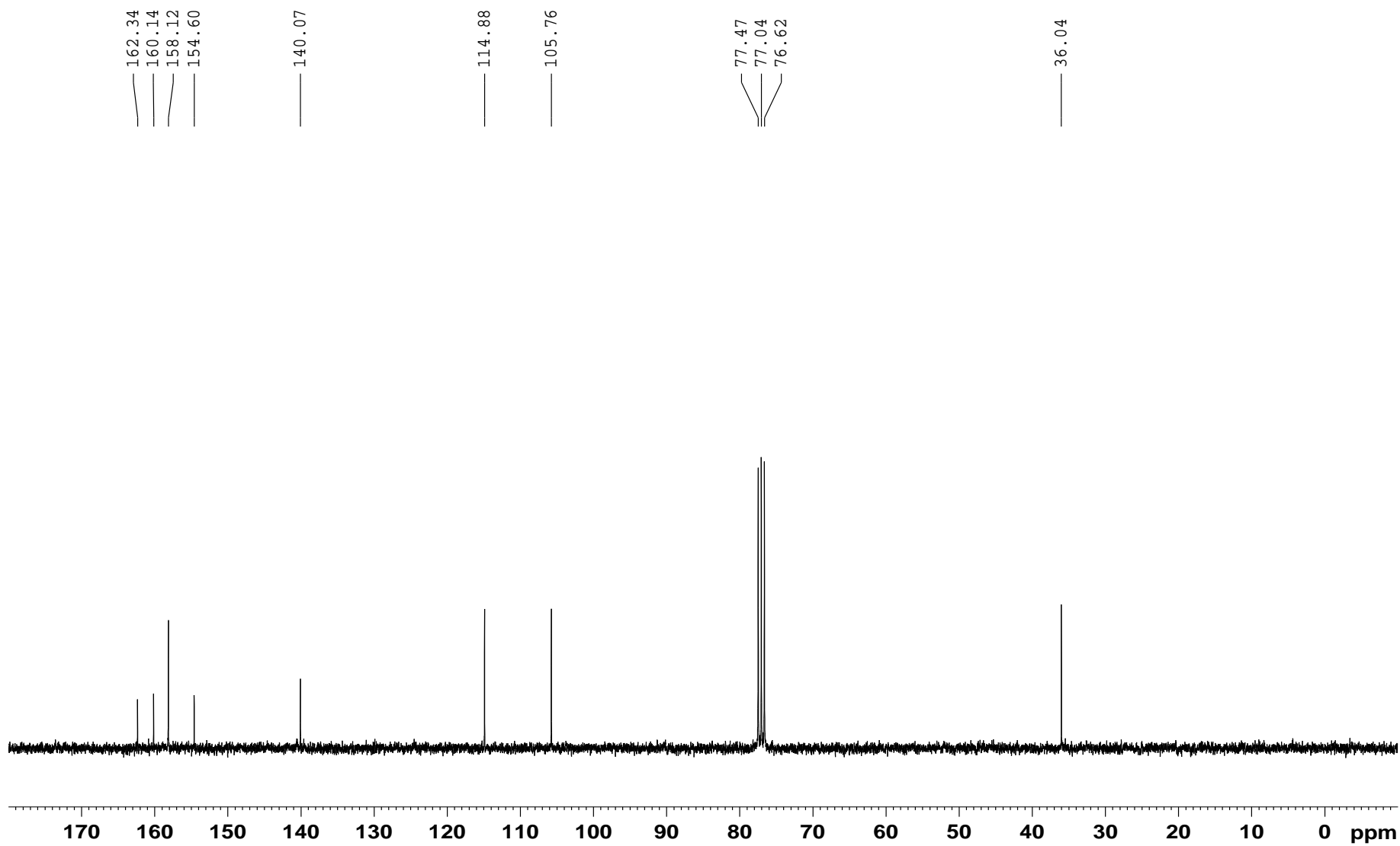
Figure S5. Mapping of the electrostatic potential onto an electron density isosurface of azacalix[3]pyridine[3]pyrimidine [B31YP/6-31g(d)]. Left: inner view. Right: outer view.

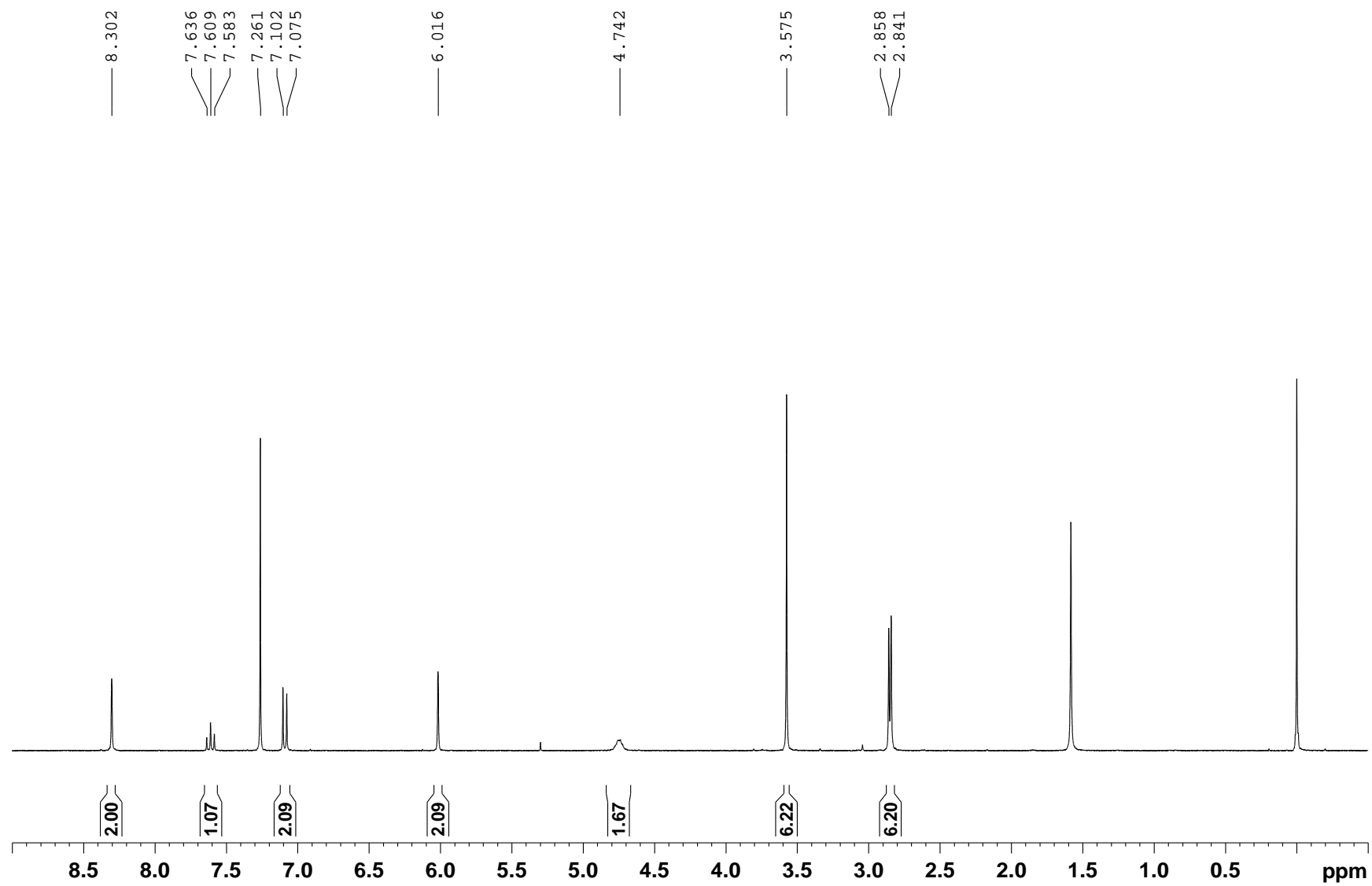
5. ^1H and ^{13}C NMR spectra of fragments 1 and 2, product 3 and pyridine and pyrimidine.

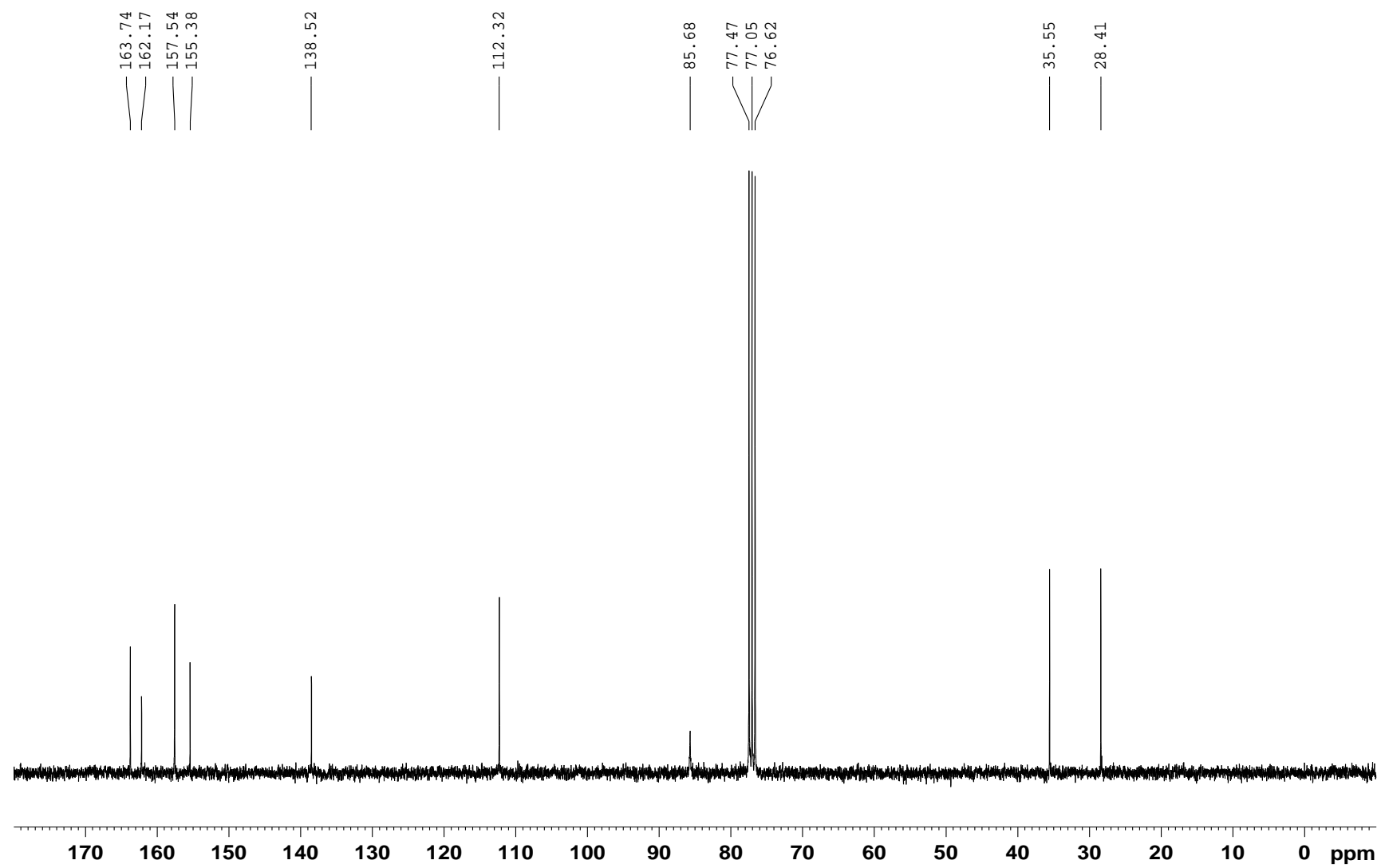


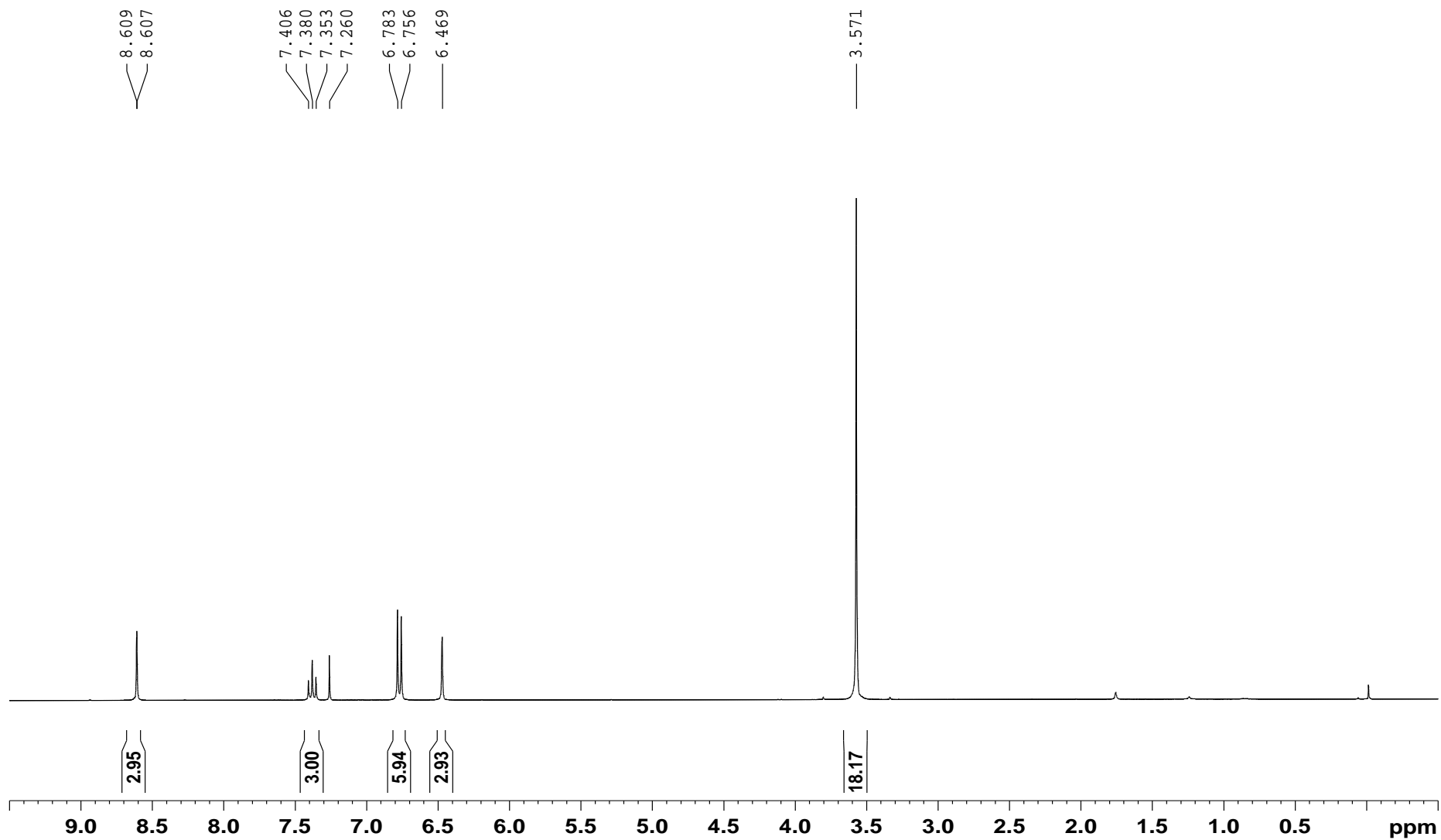


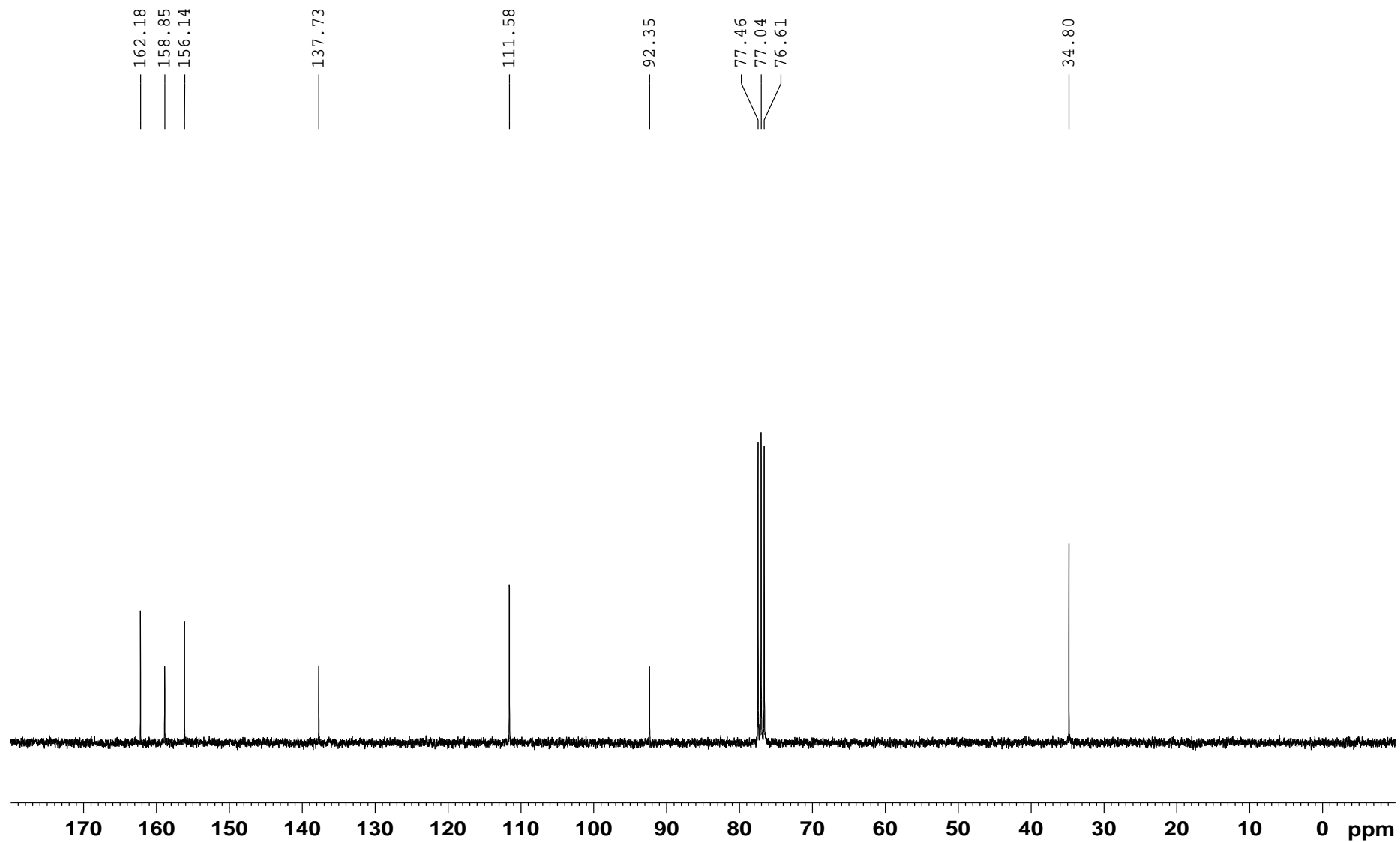












6. NMR spectra of a mixture of 3 and C₆₀ and C₇₀

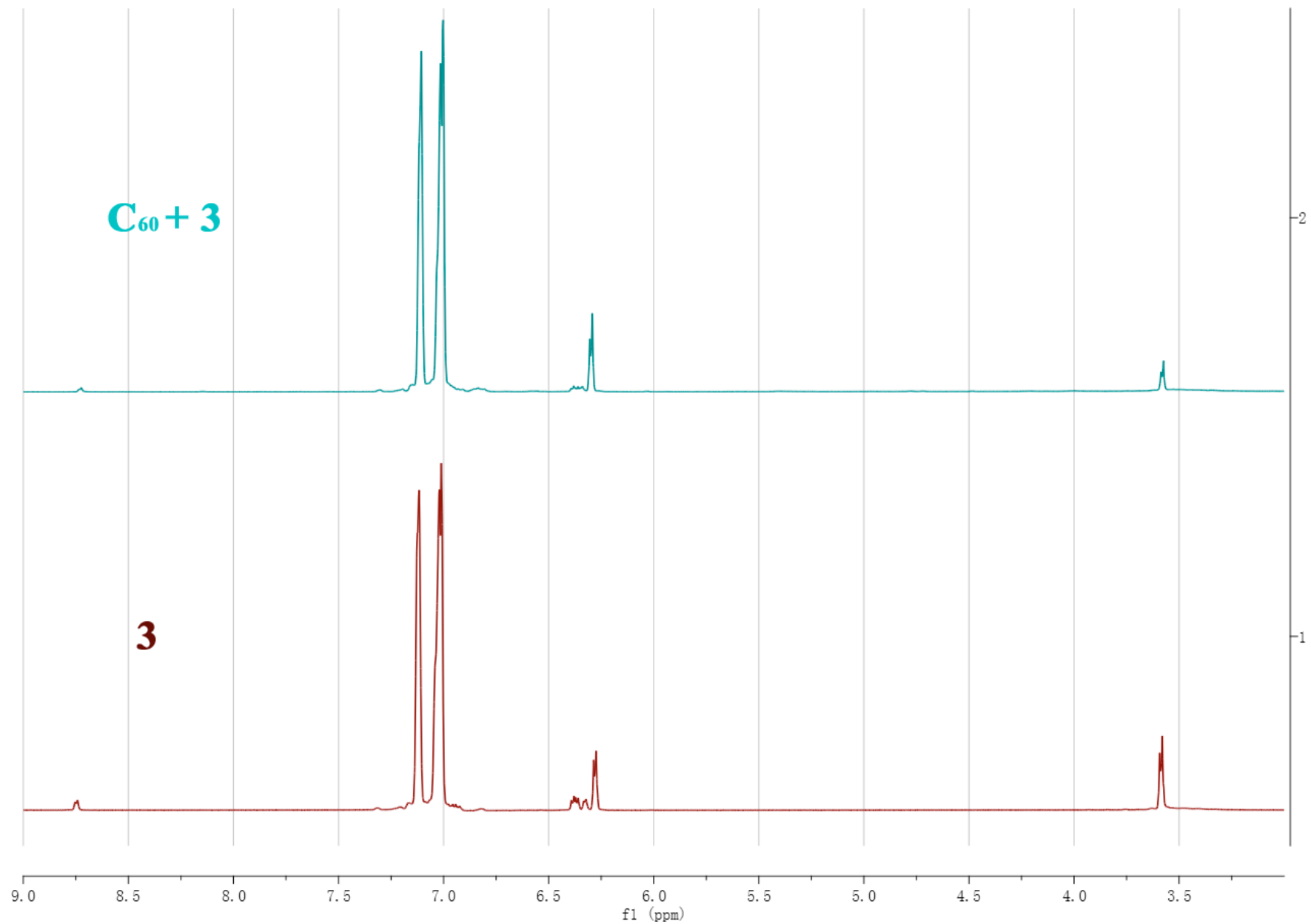


Figure S6. ¹H NMR ¹H spectrum of 3 and a 1:1 mixture of C₆₀ and 3 in *d*₈-toluene / CDCl₃ (4:1.5).

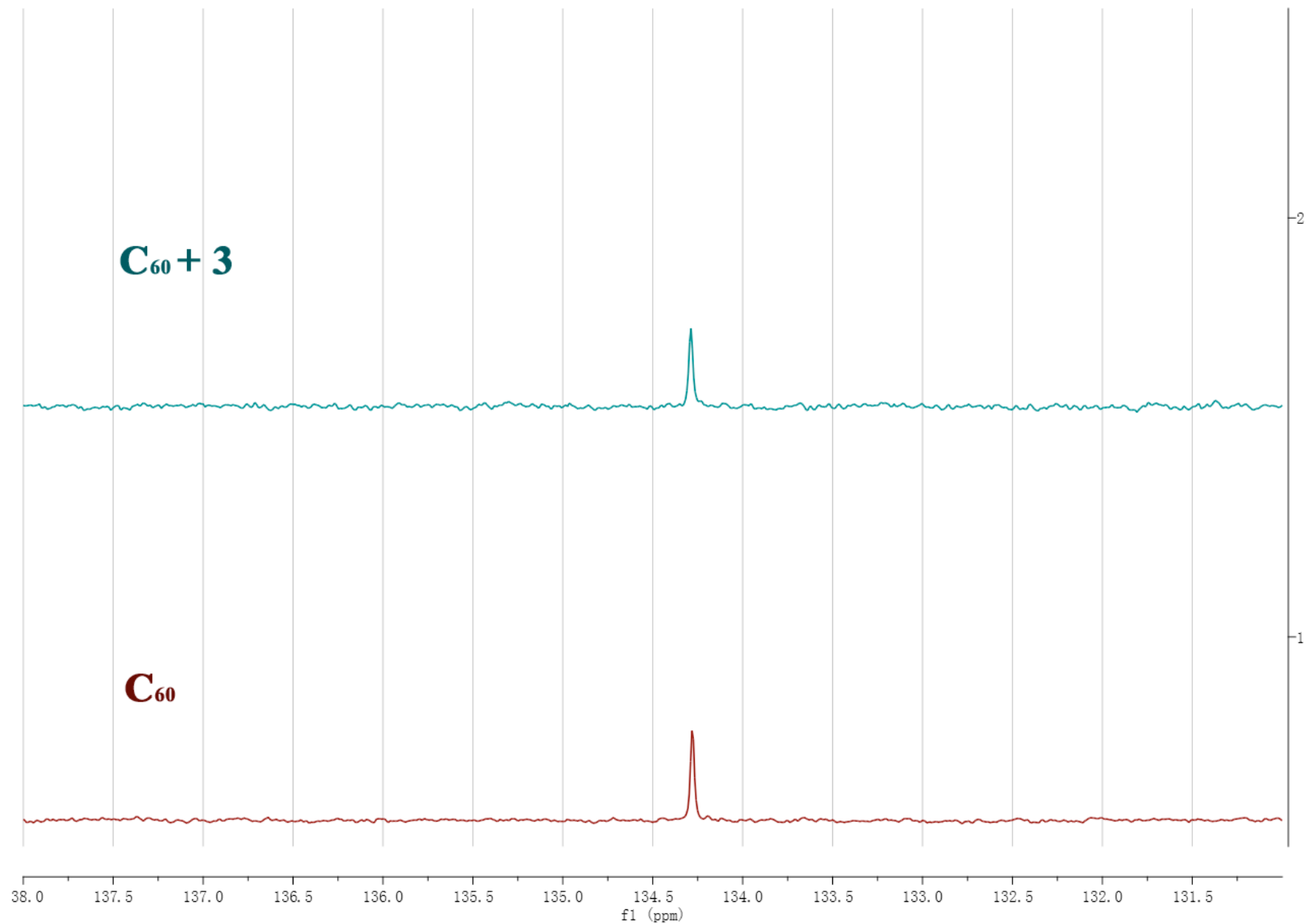


Figure S7 ^{13}C NMR spectrum of C_{60} and a 1:1 mixture of C_{60} and 3 in d_8 -toluene / CDCl_3 (4:1.5).

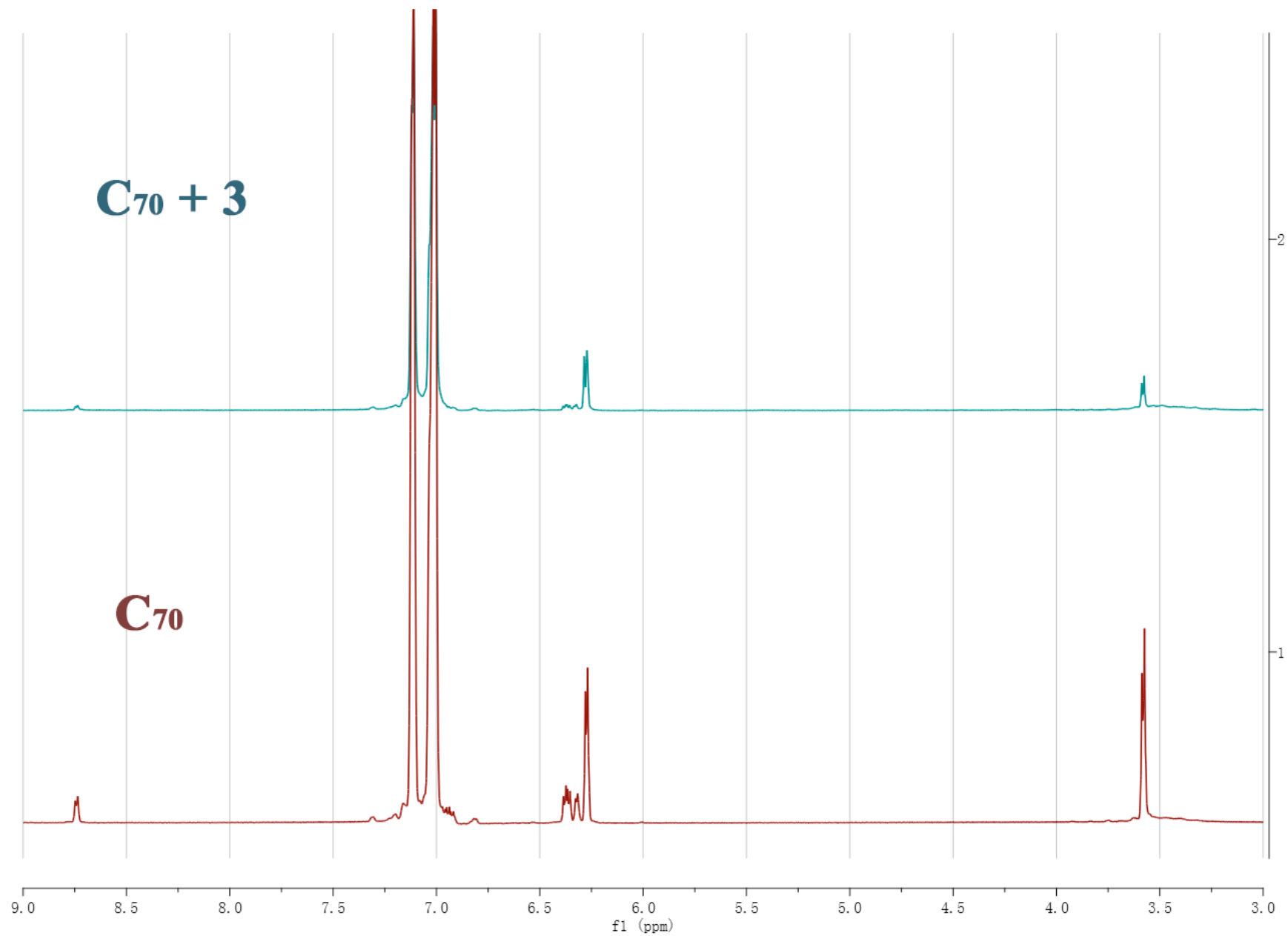


Figure S8 ¹H NMR spectrum of C₇₀ and a 1:1 mixture of C₇₀ and 3 in *d*₈-toluene / CDCl₃ (4:1.5).